Anion Exchange Membrane Functionalized by Phenol-formaldehyde Resins: Ion Exchange Capacity, Electrical Properties, Chemical Stability, Permeability, and All-iron Flow Battery

D. Parajuli, N. Murali, K. Samatha, N. L. Sahu and B. R. Sharma

Journal of Nepal Physical Society

Volume 9, Issue 2, December 2023

ISSN: 2392-473X (Print), 2738-9537 (Online)

JNPS, **9** (2): 47-55 (2023)

DOI: https://doi.org/10.3126/jnphyssoc.v9i2.62322

Published by:

Nepal Physical Society
P.O. Box: 2934
Tri-Chandra Campus
Kathmandu, Nepal
Email: nps.editor@gmail.com

JNPS 9 (2): 47-55 (2023)
ISSN: 2392-473X (Print), 2738-9537 (Online)

Research Article *© Nepal Physical Society*
DOI: https://doi.org/10.3126/jnphyssoc.v9i2.62322

Anion Exchange Membrane Functionalized by Phenol-formaldehyde Resins: Ion Exchange Capacity, Electrical Properties, Chemical Stability, Permeability, and All-iron Flow Battery

D. Parajuli[1,] *, N. Murali[2], K. Samatha[3], N. L. Sahu[4] and B. R. Sharma[5]
[1]Research Center for Applied Science and Technology, Tribhuvan University, Nepal
[2]Department of Engineering Physics, AUCE (A), Andhra University, Visakhapatnam, India
[3]Department of Physics, AUCST, Andhra University, Visakhapatnam, India
[4]Department of Physics, Tri-Chandra Multiple Campus, Kathmandu, Nepal
[5]Department of Physics, Janapriya Multiple Campus, Pokhara, Kaski
*Corresponding Email: deepenparaj@gmail.com

Received: *19th October, 2023;* ***Revised:*** *26th November, 2023;* ***Accepted:*** *22nd December, 2023*

ABSTRACT

An anion exchange membrane (AEM) is a type of selectively permeable membrane that facilitates the movement of negatively charged ions while impeding the passage of positively charged ions. These membranes are designed to selectively transport anions across them based on their charge and size. They are commonly used in various electrochemical devices and processes, such as fuel cells, electrodialysis, electrolysis, water treatment, and other applications requiring ion exchange. These membranes are typically made from synthetic polymer materials with positively charged functional groups that attract and transport anions while repelling cations. They are used for selection, conduction, and stabilizing the ion anion exchange phenomena. We recently released a study on the creation of a quick and easy approach to creating an AEM with increased ionic conduction capacity and good alkaline stability. The technique's simplicity makes it a desirable substitute for conventional methods. By using this approach, the carcinogenic reagent often employed for AEM preparation—chloromethyl methyl ether—is avoided. Membrane surfaces appeared to be rather homogeneous in Scanning Electron Microscope (SEM) pictures. Water content, ion exchange capacity, and electrical conductivity all improved as the amount of ion-exchange material in the casting fluid increased. The Thermogravimetric Analysis (TGA) of the membranes revealed thermal stability up to 150°C which shows that these membranes are ideal for applications in that temperature range. The composite membranes exhibited enhanced chemical stability in strong chemical environments and this can be attributed to the resonance stabilized guanidine group as negative ion-exchange site. By considering the AC impedance data, the conductivity measurements showed a marked enhancement in conductivity by increasing the content of ion-exchange material. Galvanostatic charged discharge tests were used to examine the electrochemical performance of an all-iron redox flow cell, and the system demonstrated a columbic efficiency of 80% during the repeated charge-discharge cycles. The findings of this work provide a compelling alternative to the established methods for the synthesis of AEMs.

Keywords: Ion exchange capacity, Electrical properties, Chemical stability, Permeability, All iron Flow battery.

1. INTRODUCTION

Rechargeable batteries and polymer electrolyte membrane fuel cells are two examples of contemporary clean energy conversion and storage technologies that are highly respected for their excellent energy conversion [1–5], low levels of noise and local pollution, and low maintenance costs. Anion-exchange membranes (AEMs) have been

thoroughly investigated by academics in recent years as separators in these devices. The limitations of Nafion-based proton exchange membrane fuel cells, including their low Carbon Monoxide (CO) tolerance, high electrokinetic overpotentials, high fuel penetration, and high catalyst costs, may be addressed by these AEMs [6–10].

The foundation polymer matrix, such as polyphenylene oxide, poly aryl ether sulfone ketones, and poly (ether ketone) (PEK), can be modified as one commonly used method for AEM production [11,12]. The typical method for adding ion-exchange groups to these membranes is a two-step procedure that involves chloro-methylating the polymers first, then exposing them to trimethylamine (TMA) to produce the appropriate trimethyl-type quaternary ammonium (QA) head group [15]. However, QA groups are susceptible to Hoffmann degradation reactions in highly alkaline environments, diminishing the durability of these membranes [16]. Moreover, AEMs produced through these methods tend to exhibit low ionic conduction capacity, rendering them unsuitable for practical applications [14]. Consequently, substantial research efforts have been dedicated to developing membranes with superior chemical stability, ionic conduction capacity, and mechanical strength [15].

Historically, the development of synthetic resins and plastics has played a crucial role in material science. In 1872, Von Bayer pioneered the creation of the first synthetic resin through the polycondensation of phenol and formaldehyde [16]. Subsequently, in 1910, Baekeland introduced the first plastic via the polycondensation of phenol and formaldehyde [13, 14]. The ion exchange property of phenol-formaldehyde (PF) resin was discovered by Adams and Holmes in 1935 [17]. Around the 1940s, synthetic ion-exchange membranes based on phenol-formaldehyde condensation products found extensive use in various industrial applications, including electrodialysis, electrodialytic concentration of seawater, and desalination of saline water [16,18–20]. Sodium phenol sulfonate, phenol, and formaldehyde were polycondensed with an alkali catalyst, phenol, and formaldehyde, to create these membranes. The condensation reaction was completed by applying a low molecular weight prepolymer to a reinforcing fabric, such as glass fiber. But it was discovered that these membranes' long-term usability was not supported by their level of durability [18-20].

Over the past two decades, significant advancements have occurred in the development of high-performance polymers for use as matrices in various types of membranes. Polyvinyl chloride (PVC) polymers have gained considerable attention due to their exceptional mechanical strength, resistance to chemicals, solubility in commonly used solvents, and widespread commercial availability. PVC-based membranes have found extensive application as battery separators, ultrafiltration membranes, and matrices in proton exchange membranes (PEM) for fuel cells [21]. J.W. Qian and colleagues achieved promising results in the pervaporation of benzene/cyclohexane mixtures using blend membranes composed of PVC and ethylene-vinyl acetate (EVA) [22]. PVC blend membranes have been created with exceptional antifouling properties by incorporating novel zwitterionic polymers into the PVC matrix. These membranes are valuable in applications where fouling is a concern [23]. Yongsheng Chen and others successfully fabricated PVC/Fe2O3 ultrafiltration membranes with excellent performance, potentially expanding their use in nanofiltration processes [24]. Our recent works on ferrites and MXenes [25] show their efficiency in the energy [1] conversion devices. These developments underscore the versatility and utility of PVC-based membranes in a wide range of applications, owing to their favorable mechanical and chemical properties.

We recently brought out a paper on the evolvement of a quick and uncomplicated approach for producing AEMs with high alkaline stability and improved ionic conduction capacity. The uncomplicated way makes it a desirable substitute for conventional methods. By using this technique, the carcinogenic chemical often utilized for AEM preparation—chloromethyl methyl ether—is avoided. SEM scans of membranes revealed a largely homogeneous surface [39]. Water content, ion exchange capacity, and electrical conductivity all improved as the weight percentage of ion-exchange material in the casting fluid increased. The findings of this work present a compelling alternative to the established methods for the synthesis of AEMs. This paper includes

2. MATERIAL, METHODS, AND CHARACTERIZATION

The previous work [26] provides a thorough explanation of all the iron flow battery studies, including the materials used, the synthesis of negative

ion-exchange material, the creation of AEM, the characterization methods, and the methodologies. Some additional techniques are as below:

Phenol, formaldehyde solution (37%), tetrahydrofuran (THF), guanidine hydrochloride, and ammonia solution were acquired from Merck. Additionally, high molecular weight commercial-grade PVC was utilized in the process.

Synthesis of anion–exchange material

Phenol and formaldehyde (in a molar ratio of 1:2) were subjected to reflux in a basic medium with a pH of 9 until a yellow resin formed and separated from the reaction mixture. This resin was removed, washed with deionized water, and dried. The resulting resin was finely powdered and dispersed in acetone, then heated with a 1-mole solution of guanidine chloride for 2 hours at 80°C. The ultimate condensation product was isolated from the reaction mixture, washed with water, filtered, and dried.

Preparation of anion–exchange membrane

A heterogeneous anion-exchange membrane was produced via the solution casting method. A specific amount of anion-exchange material and PVC powder were mixed in an appropriate solvent such as tetrahydrofuran (THF) and stirred for approximately 8 hours at room temperature. The resulting homogeneous suspension was spread onto a clean glass plate using a film applicator. After 48 hours, composite membranes with a thickness of 80 µm were peeled off from the glass plate. Before testing, all membranes were soaked in a 2M NaOH solution for 24 hours. The membrane compositions were varied by employing different quantities of guanidine functionalized anion-exchange material (10 wt%, 20 wt%, 30 wt%, and 40 wt%). These variations resulted in membranes labeled as P_1, P_2, P_3, and P_4, respectively.

Characterization Techniques

The membranes underwent characterization using FT-IR spectroscopy with Perkin Elmer spectrum two instruments (Model L160000A), covering a range from 4000 to 400 cm^{-1}. To examine the surface morphologies of the composite membranes, a scanning electron microscope (JSM-5600, JEOL Co., Japan) was utilized. Prior to microscopic examination, the samples were coated with a thin layer of gold using ion sputtering. The SEM images of the anion-exchange membranes were digitized and assessed using an image analysis system. For thermal degradation experiments of the composite membranes, a Shimadzu TGA-50 Thermo-gravimetric analyzer was employed. Thin films with an average mass of 15 mg underwent thermal analyses. The samples were subjected to heating from room temperature to 850°C under a nitrogen atmosphere at a heating rate of 10°C per minute [27].

The process to ascertain the water uptake of the composite membranes involved weighing the membranes while in a wet state after they had been stabilized in distilled water for 24 hours at room temperature. Subsequently, the membrane surfaces were meticulously dried with filter paper, and immediate weight measurements were taken. Afterward, the samples underwent vacuum drying for two days before a final weighing was conducted.

The water uptake was calculated as follows by equation (1):

$$Water\ uptake\ (\%) = \frac{W_{wet} - W_{dry}}{W_{dry}} \times 100\% \quad \text{----- (1)}$$

Where W_{wet} is the mass of the water-swollen membrane, and W_{dry} is the mass of the dry membrane.

The ion exchange capacities (IECs) of the composite membranes were established through the double titration method. Precisely weighed samples were immersed in 25 ml of 0.05 M HCl solution for 48 hours, after which the HCl solution underwent back titration using 0.05M NaOH solution with phenolphthalein as the indicator. The IECs of the samples were calculated using equation (2):

$$IEC = \frac{n_1 - n_2}{M_{dry}} \text{----------} \quad (2)$$

The calculation for the ion exchange capacity (IEC) involves using the amounts of hydrochloric acid (n_1 and n_2 in mmol) needed before and after equilibrium, along with the mass (M_{dry} in grams) of the dried sample. The average value derived from this equation across three samples represents the IEC value of the membrane.

Electrochemical impedance spectroscopy (EIS) methods were utilized to assess the ionic conductivity of the membranes, employing an AUTOLAB 50519 PGSTAT instrument. The membranes underwent impedance measurements within a two-electrode setup, sandwiched between platinum electrodes while maintaining a consistent temperature of 25±0.1°C for at least 20 minutes to ensure thermal stability. These measurements covered a frequency range of 100 Hz to 1000 kHz, applying an alternating potential with a 10 mV amplitude. Fully hydrated membranes were immersed in a conductivity cell filled with 1M

NaOH. The total resistance (R_{total}) of both the membrane and solution was measured. Additionally, the resistance of the solution alone ($R_{solution}$) was measured without the membrane. The membrane's resistance (Rmem) was derived by calculating the difference between these two resistances ($R_{mem} = R_{total} - R_{solution}$). To determine the membrane's thickness accurately, a digital micrometer was used, ensuring a flat surface and minimal compression by placing the membrane between two glass slides. The membrane's conductivity was computed as follows: $\sigma = L/RA$ mS cm^{-1}, where σ represents hydroxide conductivity in mS cm^{-1}, R denotes the ohmic resistance of the membrane (Ω), L signifies the membrane's thickness (in cm), and A stands for the cross-sectional area of the membrane samples (cm^2). For measuring methanol permeability through the membrane, a custom-made apparatus based on the Gasa method [28], derived from Walker et al. [29], was employed. This method involved sealing a specific quantity of methanol within a permeation cell and allowing it to diffuse through a membrane-covered hole of 4 cm^2 area. All measurements were conducted at room temperature. The permeation process involves the dissolution and diffusion of methanol molecules within the membrane material. The mass of methanol in the vial was monitored over time, and the membrane's permeability (P) was determined using equation (3):

$$P = \frac{N \times l}{V.P \times A \times t} \text{ ---------- (3)}$$

where N is the number of moles of methanol lost (moles), l is the thickness of the membrane, V. P. is the saturated vapor pressure of methanol at 25°C, A is the membrane area for methanol permeation in (cm^2), and t is time (days).

The assessment of alkaline stability involved immersing the composite membrane sample in a 2M aqueous NaOH solution at room temperature for a duration of 2 weeks. Subsequently, the samples were removed, washed with deionized (D.I.) water, wiped with tissue paper, and then analyzed using the FT-IR technique to identify any degradation or alterations in their chemical structures. Additionally, the loss of weight of the membrane was measured [10,30].

Regarding the oxidative stability assessment, the membrane samples sized at 3cm x 3cm were submerged in Fenton's reagent (consisting of 30 ppm FeSO4 in 30% H2O2) for 24 hours at 25°C. The evaluation involved monitoring the membrane's weight loss over time to determine its response to the exposure [31].

3. RESULTS AND DISCUSSION

3.1 Ion exchange capacity (IEC)

In Figure 1, the Ion Exchange Capacity (IEC) values of the membranes with various amounts of negative ion-exchange material are displayed. The IEC provides information on the number of changeable groups in the membrane matrix. From 0.51 to 1.23 (milimole per gram) mmol g^{-1}, the IEC values of membranes rose. With an increase in weight percent of negative ion-exchange material, it was discovered that the membrane's IEC value was rising. The Nafion 117 IEC value is 0.90 mmol g^{-1} [41]. The presence of the guanidinium cation in the membrane is responsible for the high IEC [13]. By creating interconnecting ionic conductive channels, higher IEC values promote the transit of hydroxide ions [10][42]. This will aid in the effective conduction of hydroxide ions across the membrane matrix [43].

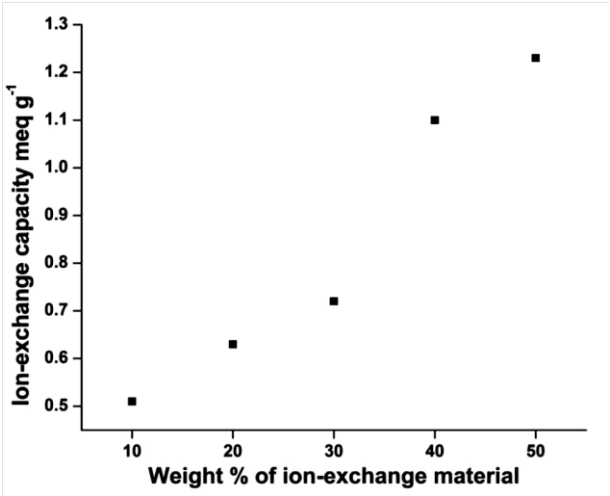

Fig. 1: Ion exchange capacity of membranes with varying negative ion-exchange material content.

3.2 Electrical properties

An important element that affects how well electrochemical devices work is the ionic conduction capacity of the AEMs. The electrochemical impedance spectra (EIS) used in this study was recorded in the frequency limit of 100 Hz to 1000 kHz and with signal amplitude of 10 mv, allowing for the examination of the ionic conductivities. As shown in Figure 2, the Nyquist plot for the AEM. The intercept on the Z' axis in the

high-frequency area of the Nyquist plot, which was used to determine membrane resistance, was obtained. Figure 3 displays the AEMs' ionic conductivities. With the rise in wt% of ion-exchange material from 10 to 40%, conductivities of AEMs increased from 11 to 71 mS cm^{-1}.

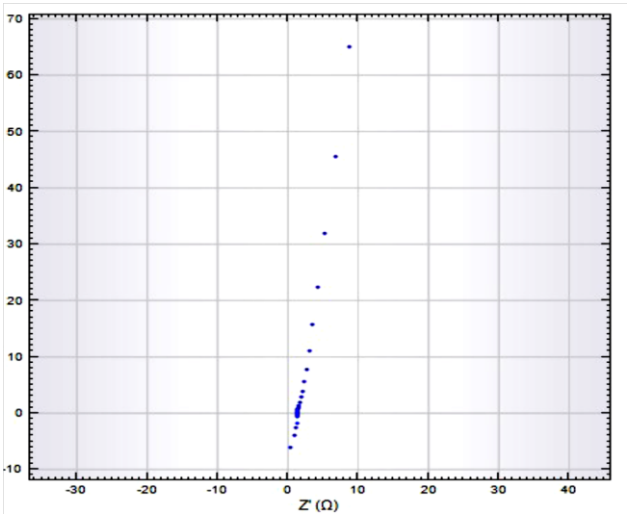

Fig. 2: Nyquist plot for the AEM P4 from AC impedance spectroscopy measurements at room temperature.

In Figure 3, the ionic conduction capacity of the fabricated membranes increases with the growing content of ion-exchange material. This demonstrates that the appropriate amount of ion-exchange material contributes to the enhancement of conductivity in the composite membranes. A uniformly dispersed hydrophilic guanidine-functionalized ion exchange material results in expanded hydrated ion transport pathways within the membrane, facilitating the conduction of anions. The increased alkalinity of the guanidinium groups has contributed to enhancing the membrane's ionic conductivity, as indicated in reference [44]. These observations are substantiated by the reason that elevation in the ion-exchange material content results in an enhanced uptake of water and an augmentation in the capacity for ionic conduction. Notably, hydroxide conduction predominantly takes place through the Grotthuss mechanism, involving the formation and rupture of bonds as they traverse the hydrogen-bonded network of water molecules (as elucidated in reference [17]). Moreover, it's important to note that the existence of hydroxyl groups on the solvated guanidinium ion exchange entities serves to enhance the inclination towards the creation and breakage of bonds in diffusing water molecules that are highly coordinated. This phenomenon can be visualized in Figure 4, where it becomes evident that as the thickness of the membrane increases, there is a decrease in the capacity for ionic conduction in the fabricated membranes.

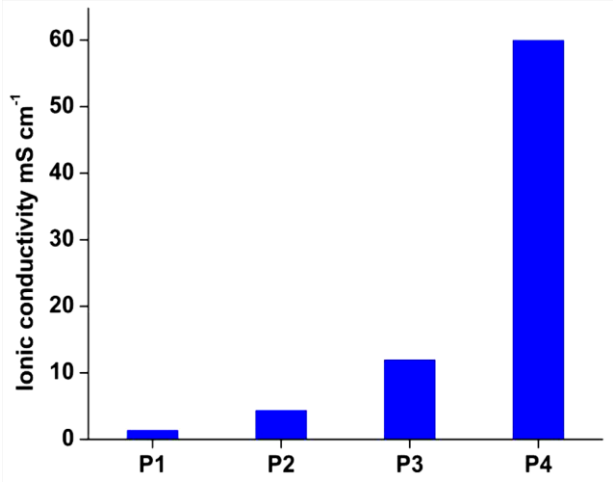

Fig. 3: Ionic conduction capacity of composite membranes Vs negative ion-exchange material wt%.

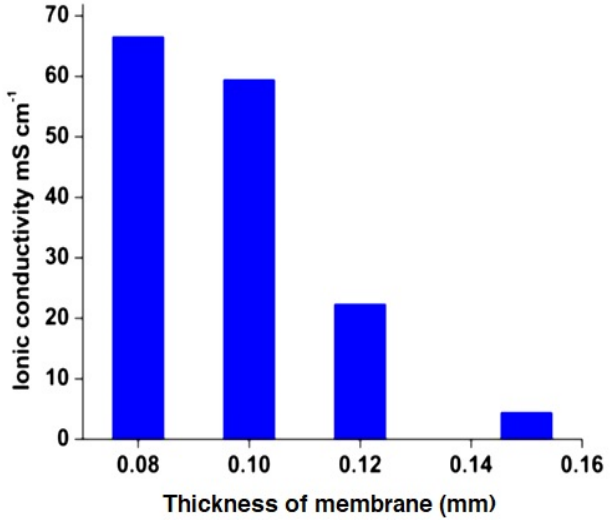

Fig. 4: Ionic conduction capacity of the composite membranes Vs. thickness.

3.3 Thermo-gravimetric analysis

The assessment of the thermal stability of these membranes involved subjecting them to Thermal Gravimetric Analysis (TGA) under a nitrogen atmosphere, with a gradual heating rate of 10°C per minute, starting from ambient temperature and reaching a maximum of 750°C. Figure 5 (a-c) provides a visual representation of the TGA profiles for (a) the PVC membrane, (b) Membrane P2, and (c) Membrane P4.

In Figure 5 (a), the initial weight reduction, amounting to under 7%, transpired during the temperature ascent from room temperature to 350°C. This diminishment was primarily a consequence of the vaporization of moisture absorbed within the sample and the liberation of pendant chloride in the form of HCl, while the underlying polyethylene backbone structure remained. The subsequent stage of weight loss emerged in the temperature range of 420 to 450°C and could be ascribed to the thermal deterioration of the polymer backbone, as indicated in reference [45]. Figure 5 (b & c) illustrates that both P2 and P4 membranes exhibit comparable degradation profiles. In the initial stage, characterized by a weight reduction of less than 7%, this decrease transpired during the temperature rise from room temperature to 250°C, primarily stemming from the evaporation of moisture absorbed within the samples. Subsequently, the second weight-loss phase, occurring between 420 and 450°C, can be ascribed to the thermal deterioration of phenyl groups and the decay of guanidinium groups present within the membranes, as discussed in reference [13]. The third stage of weight loss, which happened at temperatures exceeding 500°C, was a result of the decay of the polymer's backbone. It's worth noting that for all the membranes, weight reductions of less than 7% were observed at temperatures below 200°C, underscoring the commendable thermal stability of the fabricated membranes. This level of stability renders them highly suitable for various practical applications.

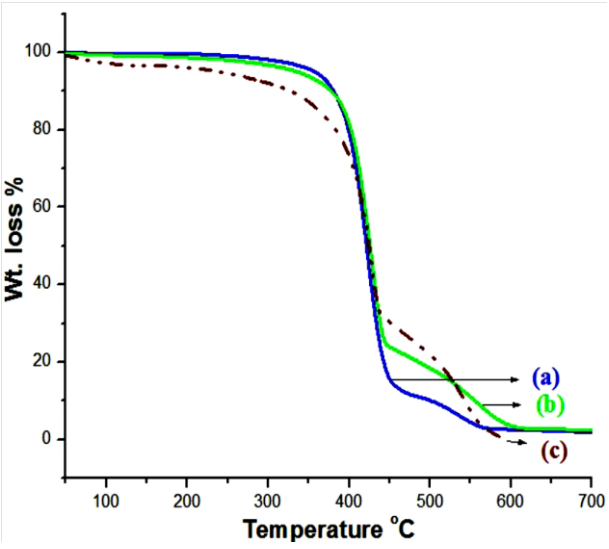

Fig. 5: TGA curves for (a) PVC membrane (b) Membrane P2 and (c) Membrane P4.

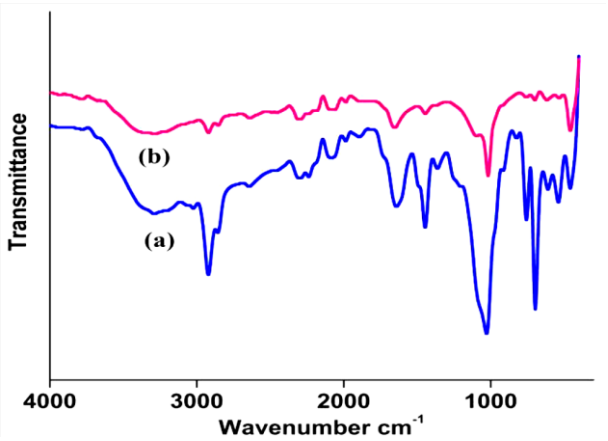

Fig. 6: FT-IR spectrum of the membrane P4 (a) before (b) after the alkaline stability test.

3.4. Chemical stability

The chemical durability of AEMs stands as a critical factor impacting the effectiveness of electrochemical devices, particularly under conditions of elevated pH and robust chemical surroundings. During a rigorous alkaline stability examination conducted over a period of two weeks in a 2M aqueous NaOH solution, all the membranes demonstrated remarkable resilience, retaining their structural integrity and flexibility. Importantly, the electrical conductivity of these membranes remained unaffected following the alkaline stability assessment, with no observable decline noted. Moreover, there was no evident degradation or loss of mass, affirming the membranes' robust and unaltered state throughout the test. This outcome underscores their reliability and suitability for extended practical use.

The examination of FT-IR data comparing the membrane before and after subjecting it to an alkaline stability test in a 2M aqueous NaOH solution provides additional compelling evidence supporting its remarkable resistance to alkaline conditions. As depicted in Figure 6, there is no discernible alteration in the intensity of absorption bands associated with C-N and -OH functional groups even after two weeks of exposure to the challenging 2M aqueous NaOH environment.

Concerns about oxidative stability consistently loom over polymer electrolyte membranes utilized in electrochemical devices, especially given the severe chemical settings they encounter. To simulate and expedite the rigorous operational conditions, Fenton's reagent is employed, generating OH- and OOH- radicals from H_2O_2 that can potentially lead to the degradation of AEMs. Notably, during this testing, all the membranes

exhibited no physical distortion or change in color, underscoring their substantial resistance to oxidation. These results substantiate the membranes' commendable resilience against oxidative challenges, reinforcing their suitability for demanding applications.

3.5. Methanol permeability

The illustration in Figure 7 depicts the methanol permeability of membranes under ambient conditions. It is evident that as the ion-exchange material content within the membrane increases, there is a progressive reduction in methanol permeability. Nevertheless, it's noteworthy that the methanol permeability exhibited by the manufactured membranes is significantly lower than that observed in the case of Nafion N117 and Tokuyama A201 membranes at room temperature, as indicated in reference [44]. Consequently, these membranes that have been synthesized generally exhibit commendable methanol barrier characteristics, as demonstrated in Figure 7.

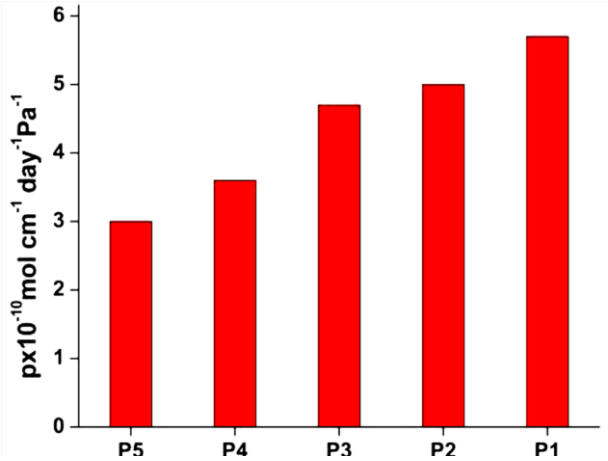

Fig. 7: Methanol permeability values of different membranes.

3.6. All iron Flow battery studies

Figure 8 displays the voltage-time curve recorded while charging and discharging an all-iron redox flow cell employing the prepared membrane as a separator. Charging was conducted at a constant current density of 100 mA cm^{-2}, whereas discharging utilized 50 mA cm^{-2}. Through numerous charge-discharge cycles at the robust current density of 100 mA cm^{-2}, it was consistently demonstrated that a high Columbic efficiency, exceeding 75%, could be upheld. This higher Columbic efficiency is indicative of minimal ion cross-mixing, as highlighted in reference [32]. These findings affirm the suitability of the novel composite membrane as an effective separator in an all-iron redox flow battery, illustrating its practical viability.

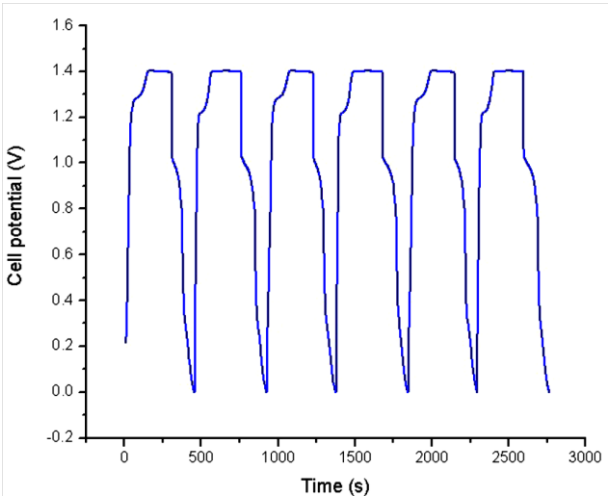

Fig. 8: The cell voltage-time curve of the all-iron redox flow cell during the galvanostatic charge-discharge experiment.

CONCLUSIONS

The IEC is found to increase with the weight percentage of ion-exchange material indicating the effective conduction of hydroxide ions across the membrane matrix. The ionic conduction capacity of the anion exchange membrane was studied with EIS for the determination of the resistance of the membrane. The ion exchange material was functionalized with uniformly dispersed hydrophilic guanidine that creates and breaks the bonds with the help of the hydroxyl group present thereby increasing water uptake. The conductivity of the AEMs was increased from 11 to 71 $mScm^{-1}$ with the increase of wt. % of ion exchange material from 10 to 40%. The ionic conductivity is decreased with the increase in thickness of the membrane. The TGA of all the membranes unveiled their thermal stability, which extended up to 200°C where the weight reduction is less than 7% indicating their applicability in this range. Furthermore, the chemical stability was checked through the alkaline test using 2M aqueous NaOH solution and Oxidative stability through Fenton's reagent test (that generates OH- and OOH- radicals from H_2O_2). The FTIR supports in drawing the conclusion that there is no distinct alteration to these membranes even under rigorous chemical conditions. The ion-exchange material content within the membrane increases, and there is a progressive reduction in methanol permeability is

decreased with the increase in the ion-exchange material within the membrane. In the evaluation of the electrochemical performance of an all-iron redox flow cell, galvanostatic charge-discharge tests were employed, with the aforementioned membrane serving as a separator. Remarkably, the system consistently exhibited a Columbic efficiency of 80% throughout repeated charge-discharge cycles. These findings present an appealing alternative to conventional methods for synthesizing AEMs, opening up new possibilities in this field of study.

REFERENCES

[1] Rambabu, C.; Aruna, B.; Shanmukhi, P. S. V.; Gnana Kiran, M.; Murali, N. et al. Effect of La3+/Cu2+ and La3/Ni2+ Substitution on the Synthesis, Magnetic and Dielectric Properties of M−type Sr1-XLaxFe12-XMxO19 (M = Cu and Ni) Hexaferrite, Inorg. Chem. Commun. **159**: 111753 (2024).

[2] Gu, C.; Huang, N.; Chen, Y.; Qin, L.; Xu, H. et al. π-Conjugated Microporous Polymer Films: Designed Synthesis, Conducting Properties, and Photoenergy Conversions, Angew. Chemie Int. Ed. **54**: 13594 (2015).

[3] Parajuli, D.; Gaudel, G. S.; KC, D.; Khattri, K. B. and Rho, W. Y. Simulation Study of TiO2 Single Layer Anti-Reflection Coating for GaAs Solar Cell, AIP Adv. **13**: 85002 (2023).

[4] Parajuli, D.; KC, D.; Khattri, K. B.; Adhikari, D. R. Gaib, R. A. and Shah, D. K. Numerical Assessment of Optoelectrical Properties of ZnSe–CdSe Solar Cell-Based with ZnO Antireflection Coating Layer, Sci. Reports 2023 131, **13**: 1 (2023).

[5] Shah, D. K.; KC, D.; Parajuli, D.; Akhtar, M. S.; Kim, C. Y. and Yang, O.-B. A Computational Study of Carrier Lifetime, Doping Concentration, and Thickness of Window Layer for GaAs Solar Cell Based on Al2O3 Antireflection Layer, Sol. Energy, **234**: 330 (2022).

[6] Zheng, J.; Zhang, Q.; Qian, H.; Xue, B.; Li, S. and Zhang, S. Self-Assembly Prepared Anion Exchange Membranes with High Alkaline Stability and Organic Solvent Resistance, *J. Memb. Sci.*, **522:** 159 (2017).

[7] Liu, L.; Tong, C.; He, Y.; Zhao, Y. and Lü, C. Enhanced Properties of Quaternized Graphenes Reinforced Polysulfone Based Composite Anion Exchange Membranes for Alkaline Fuel Cell, *J. Memb. Sci.*, **487:** 99 (2015).

[8] Shim, Y. and Kim, H. J. Nanoporous Carbon Supercapacitors in an Ionic Liquid: A Computer Simulation Study, ACS Nano, **4**: 2345 (2010).

[9] Feng, T.; Lin, B.; Zhang, S.; Yuan, N.; Chu, F. et al. Imidazolium-Based Organic–Inorganic Hybrid Anion Exchange Membranes for Fuel Cell Applications. *J. Memb. Sci.*, **508:** 7 (2016).

[10] Lin, X.; Wu, L.; Liu, Y.; Ong, A. L.; Poynton, S. D. et al. Alkali Resistant and Conductive Guanidinium-Based Anion-Exchange Membranes for Alkaline Polymer Electrolyte Fuel Cells. *J. Power Sources*, **217**: 373 (2012).

[11] Liu, Y.; Zhang, B.; Kinsinger, C. L.; Yang, Y.; Seifert, S. et al. Anion Exchange Membranes Composed of a Poly(2,6-Dimethyl-1,4-Phenylene Oxide) Random Copolymer Functionalized with a Bulky Phosphonium Cation. *J. Memb. Sci.*, **506:** 50 (2016).

[12] Tuan, C. M. and Kim, D. Anion-Exchange Membranes Based on Poly(Arylene Ether Ketone) with Pendant Quaternary Ammonium Groups for Alkaline Fuel Cell Application. *J. Memb. Sci.*, **511**: 143 (2016).

[13] Ran, J.; Wu, L.; He, Y.; Yang, Z.; Wang, Y. et al. Ion Exchange Membranes: New Developments and Applications. *J. Memb. Sci,*. **522**: 267 (2017).

[14] Merle, G.; Wessling, M. and Nijmeijer, K. Anion Exchange Membranes for Alkaline Fuel Cells: A Review. *J. Memb. Sci.*, **377**: 1 (2011).

[15] Maurya, S.; Shin, S. H.; Kim, Y. and Moon, S. H. A Review on Recent Developments of Anion Exchange Membranes for Fuel Cells and Redox Flow Batteries. *RSC Adv.*, **5**: 37206 (2015).

[16] Brydson, J. A. Plastics Materials, 920 (1999).

[17] Inamuddin and Luqman, M. Ion Exchange Technology I: Theory and Materials. *Ion Exch. Technol. I Theory Mater.* 1 (2012).

[18] Alexandratos, S. D. Ion-Exchange Resins: A Retrospective from Industrial and Engineering Chemistry Research. *Ind. Eng. Chem. Res.*, **48**: 388 (2008).

[19] Wang, Y. and Xu, T. Ion Exchange Membranes. *Encycl. Membr. Sci. Technol.* 1 (2013).

[20] Sata, T. Ion Exchange Membranes Preparation, Characterization, Modification and Application, 314 ثبثبثب **ث ققثق** (2002).

[21] Allan, J. T. S.; Prest, L. E. and Easton, E. B. The Sulfonation of Polyvinyl Chloride: Synthesis and Characterization for Proton Conducting Membrane Applications. *J. Memb. Sci.*, **489**: 175 (2015).

[22] An, Q. F.; Qian, J. W.; Sun, H. B.; Wang, L. N. Zhang, L. and Chen, H. L. Compatibility of PVC/EVA Blends and the Pervaporation of Their Blend Membranes for Benzene/Cyclohexane Mixtures. *J. Memb. Sci.*, **222**: 113 (2003).

[23] Demirel, E.; Zhang, B.; Papakyriakou, M.; Xia, S. and Chen, Y. Fe2O3 Nanocomposite PVC Membrane with Enhanced Properties and Separation Performance. *J. Memb. Sci.*, **529**: 170 (2017).

[24] Behboudi, A.; Jafarzadeh, Y.and Yegani, R. Polyvinyl Chloride/Polycarbonate Blend Ultrafiltration Membranes for Water Treatment. *J. Memb. Sci.*, **534**: 18 (2017).

[25] Parajuli, D.; Devendra, K. C.; Reda, T. G.; Sravani, G. M.; Murali, N. and Samatha, K. RHEED Analysis of the Oxidized M′2M″xXyene Sheets by Ablated Plasma Thrust Method in Pulsed Laser Deposition Chamber. *AIP Adv.,* **11**: 115019 (2021).

[26] Parajuli, D.; Murali, N.; Samatha, K.; Shah, N. L.and Sharma, B. R. Structural, Morphological, and Textural Properties of Coprecipitated CaTiO3 for Anion Exchange in the Electrolyzer. *J. Nepal Phys. Soc.*, **9**: 137 (2023).

[27] Di Vona, M. L.; Narducci, R.; Pasquini, L.; Pelzer, K. and Knauth, P. Anion-Conducting Ionomers: Study of Type of Functionalizing Amine and Macromolecular Cross-Linking. *Int. J. Hydrogen Energy*, **39**: 14039 (2014).

[28] Gasa, J. V.; Weiss, R. A. and Shaw, M. T. Ionic Crosslinking of Ionomer Polymer Electrolyte Membranes Using Barium Cations. *J. Memb. Sci.*, **304**: 173 (2007).

[29] Walker, M.; Baumgärtner, K. M.; Feichtinger, J.; Kaiser, M.; Räuchle, E. and Kerres, J. Barrier Properties of Plasma-Polymerized Thin Films. *Surf. Coatings Technol.*, **116**–**119:** 996 (1999).

[30] Lin, B.; Qiu, L.; Lu, J. and Yan, F. Cross-Linked Alkaline Ionic Liquid-Based Polymer Electrolytes for Alkaline Fuel Cell Applications. *Chem. Mater*, **22**: 6718 (2010).

[31] Wang, T.; Sun, F.; Wang, H.; Yang, S. and Fan, L. Preparation and Properties of Pore-Filling Membranes Based on Sulfonated Copolyimides and Porous Polyimide Matrix. *Polymer (Guildf).* **53**: 3154 (2012).

[32] Li, X.; Zhang, H.; Mai, Z.; Zhang, H. and Vankelecom, I. Ion Exchange Membranes for Vanadium Redox Flow Battery (VRB) Applications. *Energy Environ. Sci.*, **4**: 1147 (2011).